Earth and Planetary Science Letters xxx (2008) xxx–xxx

Contents lists available at ScienceDirect

Earth and Planetary Science Letters

journal homepage: www.elsevier.com/locate/epsl

Regular article

Controls on Messinian Lower Evaporite cycles in the Mediterranean

E.J. Rohling [a,*], R. Schiebel [a], M. Siddall [b,1]

[a] School of Ocean and Earth Science, National Oceanography Centre, Southampton SO14 3ZH, United Kingdom
[b] Department of Earth Sciences, University of Bristol, United Kingdom

ARTICLE INFO

Article history:
Received 14 May 2008
Received in revised form 12 August 2008
Accepted 18 August 2008
Available online xxxx

Editor: P. DeMenocal

Keywords:
Messinian
Mediterranean
Lower Evaporites
modelling

ABSTRACT

The Messinian Salinity Crisis in the Mediterranean, 5.96–5.33 Million years ago (Ma), represents the most recent case of massive evaporite deposition throughout an ocean basin. Here we quantitatively investigate the nature of the gypsum–marl cycles within its first phase, known as Lower Evaporites (LE) or Primary Lower Gypsum (PLG) (5.96–5.59 Ma). We conclude that to precondition the basin for deposition of the LE/PLG sequence, its connection with the open Atlantic must have been reduced to about 3% of the cross-sectional area of the modern Strait of Gibraltar. Using the modern strait morphology for scale, this would imply a connection with a depth of about 50 m and a width of several kilometres. We find that the LE/PLG evaporite–marl cycles may then have resulted from sea-level fluctuations of the order of 5 to 10 m and/or fluctuations in the Mediterranean's hydrological deficit of the order of 20%. Previous work has argued that sea-level control may be excluded, because there are too many cycles to agree with orbital obliquity-related timing. However, we argue from analogy with Quaternary sea- level records that sub-orbital sea-level fluctuations may easily reach the required magnitudes, so that sea-level control remains plausible.

© 2008 Published by Elsevier B.V.

1. Introduction

The Messinian Salinity Crisis (MSC) was characterised by massive evaporite deposition throughout the Mediterranean (Hsü et al., 1973, 1977), with estimates of the total evaporite mass ranging in the order of 6.44 to 7.88 × 10^{18} kg (Blanc, 2000, 2006). Traditionally, three phases (the 'trilogy') have been recognised within the MSC (for overviews, see Hilgen et al., 2007; CIESM, 2008), but a new and more basin-integrated view is emerging (CIESM, 2008).

A detailed elaboration of the traditional 'trilogy' concept was achieved in a recent series of key chronological and process-oriented papers about the MSC (Krijgsman et al., 1999; Krijgsman et al., 2001; Van Assen et al., 2006; Hilgen et al., 2007; and references therein) (Fig. 1A). The first phase consists of the Lower Evaporites (LE) with massive selenitic gypsum deposition in shallower regions of the Mediterranean (5.96–5.59). Then followed a widespread erosive phase that marks the apex of the MSC with widespread dessication of the basin (5.59–5.50 Ma) (Hilgen et al., 2007; Krijgsman et al., 1999; CIESM, 2008). Finally, there are the Upper Evaporites (UE; 5.50–5.33 Ma), with an intriguing mix of evaporite deposition, and a combination/alternation of both apparently marine and lacustrine depositional environments ('Lago Mare'; Hsü et al., 1973; Ruggieri and Sprovieri, 1976; McCulloch and De Deckker, 1989; Flecker et al., 2002; Hilgen et al., 2007; CIESM, 2008). Basin dessication and refill events during the UE phase have been modelled previously (Meijer and Krijgsman, 2005), as has the strontium isotope budget through the MSC (Flecker et al., 2002). Blanc (2000, 2006) developed models to investigate general changes in the depositional environment through the MSC, and the implications of inferred differentiations of evaporite deposition between different sub-basins within the Mediterranean.

The present study concerns the LE sequence, and aims to form a quantitative view of (1) the degree of basin isolation from the open ocean, and (2) the causes for the cyclic nature of the LE deposits. For context, we first summarise key features of the LE sequence from the recent series of MSC papers mentioned above (Krijgsman et al., 1999; Krijgsman et al., 2001; Van Assen et al., 2006; Hilgen et al., 2007), followed in the next section by some further constraints from the CIESM (2008) report (Fig. 1B).

The LE sequence is the first main evaporite phase of the MSC, with an onset at 5.96 ± 0.02 Ma, and a duration of 350–370 thousand years (kyr) (Krijgsman et al., 1999; Hilgen et al., 2007) (Fig. 1A). In a long-term context, the onset of the MSC is held to represent the culmination of a gradual closure of two main straits that connected the Mediterranean with the Atlantic Ocean. One was the Betic Strait through southern Spain, which closed early, in the latest Tortonian/earliest Messinian. The other was the Rifian Corridor through northern Morocco, which closed around 6.08 Ma (Krijgsman et al., 1999, 2001; Van Assen et al. 2006; CIESM, 2008). The gradual closures were tectonically driven, and recent work has rejected original proposals of superimposed restriction of water exchange through the Straits due to eustatic sea-level lowering, because the onset of the MSC coincides with a deglaciation rather than a glaciation (Hilgen et al., 2007; CIESM, 2008).

* Corresponding author.
E-mail address: e.rohling@noc.soton.ac.uk (E.J. Rohling).
[1] Currently at Lamont-Doherty Earth Observatory, 61 Route 9W — PO Box 1000, Palisades, NY 10964-8000, USA.

0012-821X/$ – see front matter © 2008 Published by Elsevier B.V.
doi:10.1016/j.epsl.2008.08.022

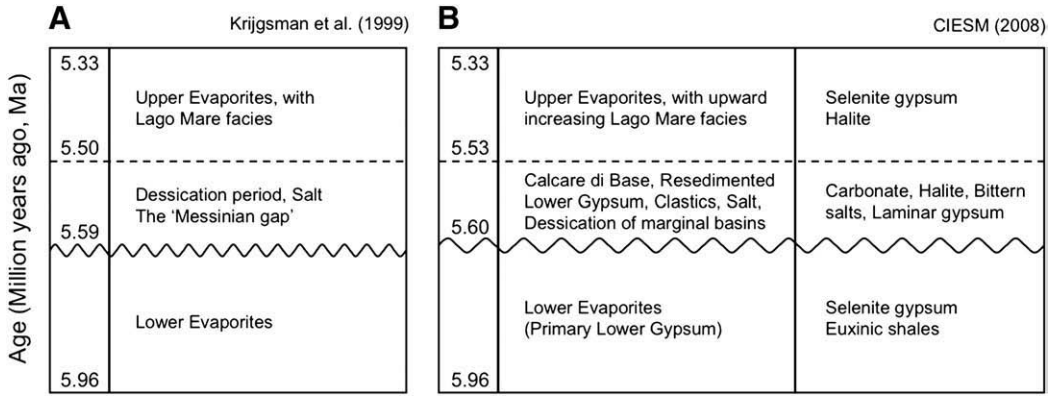

Fig. 1. Stratigraphic sequence of the Messinian Salinity Crisis. A. 'Traditional' sequence following Krijgsman and associates (Krijgsman et al., 1999; Krijgsman et al., 2001; Van Assen et al., 2006; Hilgen et al., 2007). B. Revised sequence according to CIESM (2008).

Even shallow (<200 m) basins around the Mediterranean have good LE sequence development, indicating that sea level inside the Mediterranean was not strongly drawn down by excess evaporation during its deposition (Krijgsman et al., 2001; Meijer, 2006; Hilgen et al., 2007; CIESM, 2008). This, along with the large volume of gypsum deposited, indicates that the Mediterranean retained a good connection with the open Atlantic. This would agree with the observation that, at the onset of the Lower Evaporite sequence, strontium isotope ratios were within error of Atlantic values, followed by progressive divergence from contemporary oceanic values through the deposition of the Lower Evaporites (Flecker et al., 2002). The latter may suggest a progressively increasing restriction of the Atlantic–Mediterranean connection (Flecker et al., 2002). Similar conclusions were reached by Blanc (2006).

The LE sequence contains 16–17 cycles of evaporites alternating with sapropelic (anoxic) marls (Plate 1), in an apparent 'continuation' of oxygenated marl–sapropel cycles below the LE. This may reflect a precession-regulated regional climatic control on the LE cycles, with more arid conditions leading to evaporite deposition and more humid conditions leading to sapropelic marl deposition (Krijgsman et al., 1999, 2001; Hilgen et al., 2007; CIESM, 2008).

In a box-model analysis of the LE sequence, Meijer (2006) found that basin subdivisions are generally not critical for the sequence and rapidity in which the saturation state for evaporite deposition is reached (so that evaporites would start synchronously, as dated — at least for marginal settings — to 5.96 Ma by Krijgsman et al. (1999)). Meijer (2006) also found that the rate of salinity change would allow saturation to be reached on time-scales of about 6000 years following reduction in the water exchange with the open ocean, which is fast relative to the 21.7 kyr duration of a precession cycle. Finally, Meijer (2006) argued that the evaporite sequence is not thick enough to be explained fully by a 'blocked outflow' scenario, as that would cause about twice the observed thickness of evaporites. Hence, Meijer (2006) concluded that some outflow of brine from the Mediterranean

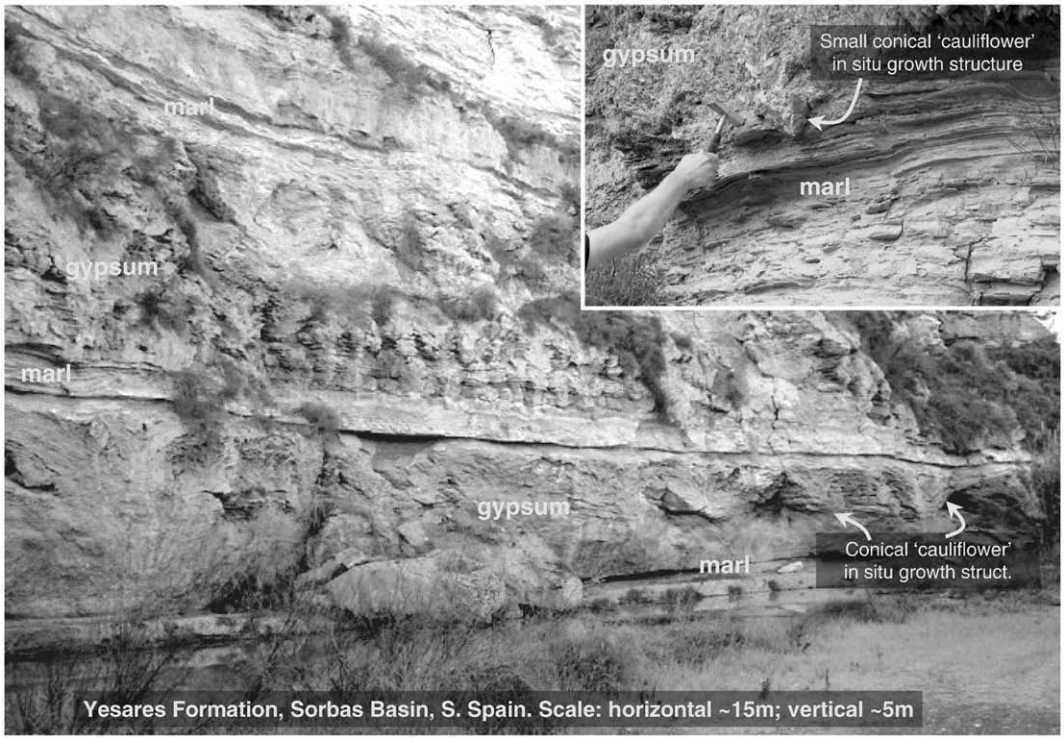

Plate 1. Photograph of gypsum–marl cycles in the Yesares Formation in Sorbas Basin, Southern Spain. Conical 'cauliflower' in-situ growth structures can be seen in the selenitic gypsum beds. Main photograph by A.P. Roberts, inset by E.J. Rohling.

Please cite this article as: Rohling, E.J., et al., Controls on Messinian Lower Evaporite cycles in the Mediterranean, Earth Planet. Sci. Lett. (2008), doi:10.1016/j.epsl.2008.08.022

ARTICLE IN PRESS

must (at times) have prevailed, thus contradicting Blanc's (2000, 2006) deduction that outflow was reduced to nil.

Despite the progress in quantitative understanding of the LE sequence discussed above, there remain two unexplored aspects, which we address in the present paper. The first concerns the level of restriction of the Mediterranean from the Atlantic during the LE phase. Although the Betic and Rifian straits are both documented to have closed at least 120 kyr before the onset of the MSC, the 'connected' nature of the Mediterranean during the LE deposition indicates that at these early stages some (residual?) connection with the Atlantic must have persisted somewhere (see also Blanc, 2000, 2006). In short, the first fundamental question we ask is: What would have been the connection's likely dimensions? The second key question concerns the nature of the cyclic deposits in the LE sequences: What magnitude of climate and/or sea-level variability would be needed to force cycles from 'normal' marine conditions with sapropelic marl deposition, to hypersaline conditions with gypsum deposition, and what is the feasibility of such variability?

Because there are no constraints on the dimensions of any connecting strait to the Atlantic at the time of the LE deposition, we formulate our arguments by considering the changes that would have to occur to the present-day Mediterranean to create the observed type of cyclic deposits. Strait restriction may then be expressed in terms of an equivalent water-depth reduction in the modern Strait of Gibraltar. Although such a 'what if' approach does not provide a detailed palaeoceanographic reconstruction, it does help to conceptualise the magnitudes and thus the feasibility of the changes in the basin's forcing needed to generate the observed cyclic deposits. By developing the arguments completely in a relative sense (relative to the present), we avoid speculating on the past magnitudes of crucial fluxes and dimensions, which are poorly known.

2. More specific identification of the interval of interest

Although the interval of study has long been known as the Lower Evaporites, a clear understanding of which types of evaporite sediments are involved in this phase throughout the Mediterranean requires that we follow the more specific constraints clarified in a recent multi-author consensus document (CIESM, 2008) (Fig. 1B). This report redefines the LE sequence, with its 16/17 precession cycles, as Primary Lower Gypsum (PLG; 5.96–5.60 Ma), which consists of gypsum deposits in shallower settings, and euxinic shales in the deep basins. The CIESM (2008) report ascribes the absence of gypsum in the euxinic shales to inhibition of gypsum formation by the euxinic bottom water conditions, or possibly to less concentrated deep brines. Crucially, the report clarifies that there is no halite associated with the PLG. The PLG deposition was followed by dessication of the basin, leading to deep canyon incisions and other widespread erosion, as well as formation of primary evaporites that include halite and potash salts along with widespread Resedimented Lower Gypsum (RLG) units (CIESM, 2008) (Fig. 1B). Finally, the report argues that the Upper Evaporites were formed from 5.53 Ma, until the Pliocene flooding of 5.33 Ma.

The present paper concerns the PLG deposits with 16/17 (precession) cycles from sapropelic marl to gypsum. These deposits comprise gypsum, but no halite.

3. Method

We develop a set of basic equations that govern the volume transport and properties of exchange between the Atlantic and the Mediterranean (see schematic in Fig. 2, and list of parameters in Appendix A). We start with the simple relationships associated with conservation of mass and salt (Nielsen, 1912):

$$\begin{aligned} Q_a S_a &= -Q_m S_m \\ Q_a &= -Q_m - X \\ S_m - S_a &= \Delta S \end{aligned} \qquad (1)$$

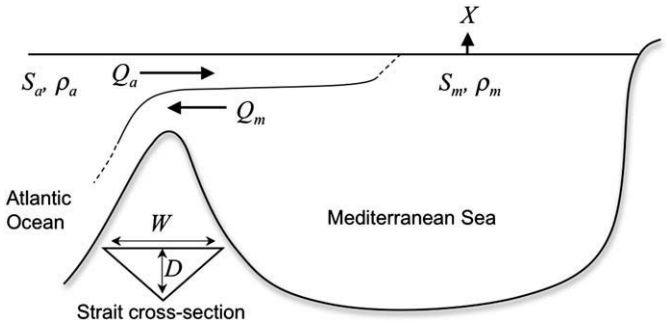

Fig. 2. Schematic of the system considered in the present paper. The inset illustrates the fundamentally triangular strait cross section (BK91). Symbols are explained in the text, and listed in Appendix A. We use a one-basin representation for the Mediterranean, following Meijer's (2006) conclusion that basin subdivisions are generally not critical for the sequence and rapidity in which the saturation state for evaporite deposition is reached.

where Q_a (S_a) is inflow volume transport (salinity) of Atlantic water into the Mediterranean, Q_m (S_m) is outflow volume transport (salinity) of Mediterranean water into the Atlantic, and X is the excess of evaporation over total freshwater input (precipitation, runoff, and net freshwater flux from the Black Sea). Conservation of salt is an assumption that may not be fulfilled, especially during periods of known evaporite (notably halite) deposition. We discuss in the next section ('Application') how salt precipitation would affect the solutions (part 2 of Appendix A gives the modified equations). Because $-Q_m = Q_a + X$, the relationships in Eq. (1) give

$$Q_a = X\left(\frac{S_m}{\Delta S}\right). \qquad (2)$$

Any inflow volume in the past ($Q_{a(1)}$) can then be expressed as a fraction relative to the value of inflow volume in modern times ($Q_{a(0)}$) as

$$f_{Q_a} = \frac{Q_{a(1)}}{Q_{a(0)}} = \frac{X_{(1)}}{X_{(0)}} \cdot \frac{\left(\frac{S_{m(1)}}{\Delta S_{(1)}}\right)}{\left(\frac{S_{m(0)}}{\Delta S_{(0)}}\right)} \quad \text{or} \quad f_{Q_a} = \frac{X_{(1)}}{X_{(0)}} \cdot \frac{S_{m(1)}}{S_{m(0)}} \cdot \frac{(S_{m(0)} - S_{a(0)})}{(S_{m(1)} - S_{a(1)})}. \qquad (3)$$

We assume that the open oceanic inflow salinity does not change ($S_{a(1)} = S_{a(0)}$), where the modern value is $S_{a(0)} = 36.2$, while $S_{m(0)} = 38.3$ so that $\Delta S_{(0)} = 2.1$ (Bryden and Kinder, 1991). We also assume that the basin reaches steady state, which is reasonable since this occurs within about 6 kyr, so that there is ample time within a 21.7 kyr precession cycle (see Meijer and Krijgsman, 2005; Meijer, 2006). We then find:

$$f_{Q_a} = \frac{X_{(1)}}{X_{(0)}} \cdot \frac{S_{m(1)}}{38.3} \cdot \frac{2.1}{(S_{m(1)} - 36.2)} \quad \text{so that} \quad f_{Q_a} = f_X \cdot \frac{0.05483}{\left(1 - \frac{36.2}{S_{m(1)}}\right)} \qquad (4)$$

where f_X represents the ratio of past excess evaporation relative to its present-day value ($X_{(1)}/X_{(0)}$). The relationships for conservation of mass and salt used in the above do not account for the reasons why Q_a would change when X and/or S_m (hence ΔS) change, or — crucially — for the influences of changes in the strait configuration. Those relationships, however, are considered in hydraulic exchange models for the strait, and for Gibraltar, a suitable model is that of Bryden and Kinder (1991) (hereafter BK91). Using that model, we can develop a set of complementary equations to (4), which will lead to a unique solution for the relationship between f_X and S_m relative to the configuration of the modern strait at different water depths over the sill. Sill depth may be both isostatically and eustatically affected.

The BK91 model calculates exchange transports as a function of the cross-sectional area of the strait, and of the density contrast between the Atlantic and the Mediterranean, which BK91 express in terms of the salinity difference using $\rho_m = \rho_a + \beta \Delta S$ (which assumes a simple

Please cite this article as: Rohling, E.J., et al., Controls on Messinian Lower Evaporite cycles in the Mediterranean, Earth Planet. Sci. Lett. (2008), doi:10.1016/j.epsl.2008.08.022

linear relationship between temperature and salinity). The strait is represented as having a triangular cross section, in close agreement with the actual strait profile (BK91). The model assumes that the exchange is critical today. Some studies suggest that the modern exchange may be marginally sub-critical (Bormans and Garrett, 1989a; Garrett et al., 1990), but for periods of significant sill depth reduction the assumption of critical exchange likely is correct (Siddall et al 2002, 2004; Matthiesen and Haines, 2003). Some studies have considered the effects of rotation and tides on the exchange (Bormans and Garrett 1989a,b), but given the success of models that neglect these relatively subtle effects (BK91) and the reduction of the width of the strait during periods of reduced sill depth, we consider that the effects of tides or rotation do not significantly affect our results. The present study concerns approximate estimates of large changes in the exchange fluxes during periods when changes in the exchange are dominated by the impacts of strongly reduced water depths in the strait. For our first-order assessments, therefore, the assumption of critical exchange, and neglect of rotation and tides, are sufficient.

The BK91 model also excludes any impacts of friction between inflow and outflow. The calculations for the greatest strait depth reduction in the present study may be somewhat affected by this, and actual exchange transports may be somewhat smaller than simulated (Bormans and Garrett 1989a). However, Pratt (1986) found the Strait of Gibraltar the least likely of all straits considered in his study to show frictional impacts on the exchange. Indeed, simple hydraulic models that neglect the effect of friction on the exchange fluxes successfully provide accurate estimates of the exchange fluxes (BK91). Analogy with Red Sea exchange models suggests that the friction impacts would be limited even in our case of strongest strait depth reduction, leaving about 40 m of water above the sill (Siddall et al., 2004; Biton et al., 2008). The BK91 model finds that total exchange transport through the strait is expressed as

$$Q_{tot}=C\cdot\frac{WD}{2}\cdot\sqrt{\frac{gD\beta\Delta S}{\rho_m}} \tag{5}$$

where W is the width and D the depth of the strait cross section, C is a constant, g the acceleration due to gravity, and $Q_{tot}=Q_a-Q_m=2Q_a+X$. Reorganisation of Eq. (2) to solve for X gives

$$X=Q_a\left(\frac{\Delta S}{S_m}\right)\quad\text{so that}\quad Q_{tot}=Q_a\left(2+\frac{\Delta S}{S_m}\right). \tag{6}$$

Substitution of Eq. (6) into Eq. (5) gives

$$Q_a=\frac{C\cdot\frac{WD}{2}\cdot\sqrt{\frac{gD\beta\Delta S}{\rho_m}}}{\left(2+\frac{\Delta S}{S_m}\right)}. \tag{7}$$

We can now use f_{Q_a} to express a past $Q_{a(1)}$ relative to the modern $Q_{a(0)}$, which gives

$$f_{Q_a}=\frac{Q_{a(1)}}{Q_{a(0)}}=\frac{C\cdot\frac{W_{(1)}D_{(1)}}{2}\cdot\sqrt{\frac{gD_{(1)}\beta\Delta S_{(1)}}{\rho_{m(1)}}}}{\left(2+\frac{\Delta S_{(1)}}{S_{m(1)}}\right)}\cdot\frac{\left(2+\frac{\Delta S_{(0)}}{S_{m(0)}}\right)}{C\cdot\frac{W_{(0)}D_{(0)}}{2}\cdot\sqrt{\frac{gD_{(0)}\beta\Delta S_{(0)}}{\rho_{m(0)}}}}. \tag{8}$$

Following BK91, we use $\rho_m=\rho_a+\beta\Delta S$. Thus, Eq. (8) becomes

$$f_{Q_a}=\frac{W_{(1)}D_{(1)}\sqrt{D_{(1)}}}{W_{(0)}D_{(0)}\sqrt{D_{(0)}}}\cdot\frac{\left(2+\frac{\Delta S_{(0)}}{S_{m(0)}}\right)}{\left(2+\frac{\Delta S_{(1)}}{S_{m(1)}}\right)}\cdot\sqrt{\frac{\Delta S_{(1)}}{\Delta S_{(0)}}\cdot\frac{\left(\rho_{a(0)}+\beta\Delta S_{(0)}\right)}{\left(\rho_{a(1)}+\beta\Delta S_{(1)}\right)}}. \tag{9}$$

Given a triangular strait profile (BK91), W and D reduce proportionally to one another. We take n to represent the ratio of past over modern W and D, so that $n=W_{(1)}/W_{(0)}=D_{(1)}/D_{(0)}$. The left-hand term in Eq. (9), which represents the influence on inflow exerted by a change in the cross-sectional area of the strait, then reduces to $n^{5/2}$. To consider an example, for any reduction in water depth in the strait to 44% of the present-day value (i.e., sea-level drop amounting to 56% of the sill depth, or strait uplift to the point that the strait is only 44% as deep as today), n would be 0.44.

As before, we assume no changes in the inflowing water properties, so that $\rho_{a(1)}=\rho_{a(0)}$. Note that $\Delta S_{(1)}=S_{m(1)}-S_{a(1)}=S_{m(1)}-S_{a(0)}$. We can then fill in the known values. Note that, for clarity, we here follow as close as possible BK91, who express the various density terms in g cm^{-3} rather than kg m^{-3}. With $\beta=0.77\times10^{-3}$ g cm^{-3} ppt^{-1} (BK91) and $\rho_{a(0)}=1.027$ g cm^{-3} (Bryden and Stommel, 1984), Eq. (9) becomes

$$f_{Q_a}=n^{5/2}\cdot\frac{2.05483}{\left(3-\frac{36.2}{S_{m(1)}}\right)}\cdot\sqrt{\frac{1.02862}{\left(\frac{2.153}{S_{m(1)}-36.2}+1.62\times10^{-3}\right)}} \tag{10}$$

so that

$$n=\left(\frac{f_{Q_a}}{\frac{2.05483}{\left(3-\frac{36.2}{S_{m(1)}}\right)}\cdot\sqrt{\frac{1.02862}{\left(\frac{2.153}{S_{m(1)}-36.2}+1.62\times10^{-3}\right)}}}\right)^{2/5}. \tag{11}$$

We can now equate Eqs. (4) and (10):

$$f_{Q_a}=f_X\cdot\frac{0.05483}{\left(1-\frac{36.2}{S_{m(1)}}\right)}=n^{5/2}\cdot\frac{2.05483}{\left(3-\frac{36.2}{S_{m(1)}}\right)}\cdot\sqrt{\frac{1.02862}{\left(\frac{2.153}{S_{m(1)}-36.2}+1.62\times10^{-3}\right)}} \tag{12}$$

so that

$$f_X=\frac{2.05483}{0.05483}\cdot n^{5/2}\cdot\frac{(S_{m(1)}-36.2)}{(3S_{m(1)}-36.2)}\cdot\sqrt{\frac{1.02862}{\left(\frac{2.153}{S_{m(1)}-36.2}+1.62\times10^{-3}\right)}}. \tag{13}$$

Eq. (13) allows us to explore the relationship between f_X and $S_{m(1)}$ for different sill depths (n) (Fig. 3). Thus, we can evaluate whether, with

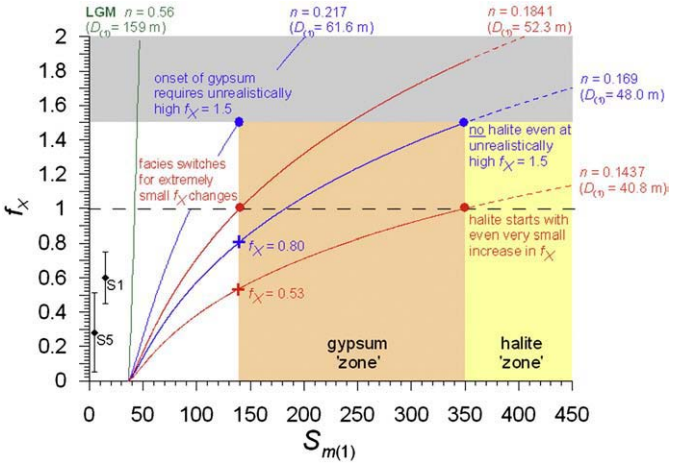

Fig. 3. Results from Eq. (13), showing the relationship between salinity in the Mediterranean basin ($S_{m(1)}$) and the ratio of excess evaporation relative to the present value $f_X=X_{(1)}/X_{(0)}$), for a range of different values of sill depth reduction, relative to the present ($n=D_{(1)}/D_{(0)}$). Reported values of $D_{(1)}$ indicate the past water depth over the sill. The green line gives the relationship for the Last Glacial Maximum configuration with sea-level lowering of 125 m (i.e., $n=0.56$ so that $S_{m(1)}=42.3$ at $=1.0$) (Fairbanks 1989, 1990). The upper blue line ($n=0.217$) reaches saturation for gypsum at the highest realistic value of $f_X=1.5$ (see text). The upper red line ($n=0.1841$) reaches gypsum saturation for $f_X=1.0$ ($S_m=140$). The lower blue line ($n=0.169$) reaches saturation for halite ($S_m=350$) at the highest realistic value of $f_X=1.5$ (see text). The lower red line ($n=0.1437$) reaches halite saturation for $f_X=1.0$ ($S_m=350$). Four 'critical transition points' in the plots are identified with red and blue dots, with brief descriptions. Crosses identify the reductions of f_X needed in two key scenarios to cause transition between predominant gypsum or marl precipitation. For comparison, the black diamonds with uncertainty limits illustrate the reductions of f_X reconstructed previously for the orbital precession-induced humid periods that mark Holocene sapropel S1 (Rohling, 1999) and Last Interglacial Sapropel S5 (Rohling et al., 2004b).

Please cite this article as: Rohling, E.J., et al., Controls on Messinian Lower Evaporite cycles in the Mediterranean, Earth Planet. Sci. Lett. (2008), doi:10.1016/j.epsl.2008.08.022

Table 1
Values for the ratio of inflow relative to its modern value ($f_{Q_a} = Q_{a(1)}/Q_{a(0)}$) for key values of $S_{m(1)}$, based on excess evaporation equal to the present ($f_X = 1.0$), from Eq. (4)

'Event'	$S_{m(1)}$	f_{Q_a} at $f_x = 1.0$	n	Sill depth (m)
LGM	42.3	0.3818	0.5598	159.0
Onset of gypsum	140.0	0.0740	0.1841	52.3
Onset of halite	350.0	0.0612	0.1437	40.8

Similarly, values of sill depth reduction relative the present ($n = D_{(1)}/D_{(0)}$), from Eq. (11). The depth of water over the sill equals n times the modern sill depth (284 m, see BK91).

a restricted strait (low n), $S_{m(1)}$ might vary sufficiently to change between evaporite lithofacies (as observed in the Lower Evaporites) in relation to realistic changes in the net hydrological deficit of the basin.

4. Application

Although in an evaporative setting gypsum may initially start to precipitate from normal sea water ($S = 35$) after water volume reduction by a factor 3 to 3.3 ($S = 110$) (e.g., Bitzer, 2004 and references therein), it is generally considered to become dominant when the water volume is reduced by a factor 4; that is, to about 25% or less (equivalent to an increase from the original salinity to $S > 140$). Halite becomes dominant when the water volume is reduced to about 10% or less (equivalent to $S > 350$), and bittern salts when the volume is reduced to about 5 to 3% and less.

The current paper focuses on the range of gypsum precipitation and the transition to halite, where the simple salinity values can be used as a reasonable approximation of the concentration effect. For the onset of gypsum, we use $S = 140$, and for the transition to halite we use $S = 350$. Use of these values allows easy comparison with previous studies (e.g., Flecker et al., 2002; Meijer and Krijgsman, 2005; Meijer, 2006), but we note that the value used for the onset of gypsum precipitation may exceed the real saturation point (Bitzer, 2004 and references therein). Table 1 lists some critical values calculated using constant excess evaporation ($f_X = 1.0$), which illustrate that a severe reduction in inflow (to 7.4% of the present value) is needed to achieve gypsum saturation, which implies a sill depth of about 52 m, while only minor further reduction (to 6.1%) would lead to the onset of halite precipitation (sill depth about 41 m).

Before exploring the relationships in more detail, we note two caveats to the use of our model. First, when friction becomes non-negligible, at low sill depths, exchange transports will tend to be somewhat smaller than calculated for a given n, so that salinity contrasts would be somewhat larger than calculated. Hence, inclusion of friction would cause salinity thresholds to be achieved at somewhat larger sill depths than calculated above. Effectively, this would displace the curves slightly downward in Fig. 3. This caveat is important in the case of the potentially very long and shallow Messinian connection(s), where more impact of friction may be expected than in the geometry of the modern Strait of Gibraltar. Second, when salt precipitation becomes very important (notably when halite precipitates), the equations for salt conservation shown in Eq. (1) would need adaptation by inclusion of a salt deposition term on the right-hand side (see Appendix A). This would slightly reduce the increase of $S_{m(1)}$, offsetting the curves at $S > 350$ somewhat in an upward direction from their position in Fig. 3. This effect is negligible in the range of salinities up to the point of NaCl saturation at $S = 350$, and remains small even above that (see Appendix A). Consequently, the calculated curves are not modified, but to account for this slight bias they are drawn solid up to $S = 350$, and dashed for $S > 350$. Note that the potential impacts of our two main caveats work in opposite directions, and thus — to some extent — cancel out against one another.

5. Discussion and conclusions

Fig. 3 reveals that, for the modern Mediterranean to develop conditions similar to the LE/PLG, with abundant gypsum that alternates with sapropelic marls, but with no halite, sill depth should be reduced to within a range of about 50 ± 10 m. Given the unlikely condition that f_X would become larger than 1.5 and the limitation that no halite should precipitate, the most likely range for sill depth would be about 48 + 5/−7 m (see below). Note that a change in f_X to 1.5 would correspond in scale to a complete cessation of all freshwater input into the basin from rivers and from the Black Sea.

Assuming a constant sill depth of 48 m at $f_X = 1.0$, which would sustain the basin well within the gypsum saturation range, a sea-level rise of only 5 m or more (to $n > 0.184$) at constant f_X would have the potential to change the deposition to marls. From the same starting point, a sea-level drop of only 7 m or more (to $n < 0.144$) at constant f_X would have the potential to change the dominant evaporite deposition to halite, which is not observed in association with the LE/PLG (CIESM, 2008). This suggests that sea-level control on the LE/PLG evaporite cycles would be highly feasible, and given that even Quaternary studies cannot constrain sea level with uncertainties much better than ±5 m (e.g., Fairbanks, 1989, 1990; Waelbroeck et al., 2002; Siddall et al. 2003, 2004, 2006, in press; Rohling et al., 2004a, 2008), any such Messinian sea-level control might be undetectably small.

With $n = 0.169$ (a sill depth of 48 m), the strait's cross-sectional area would have been reduced by a factor n^2 to about 3% of that of the modern Strait of Gibraltar. Clearly, a small (residual) opening would have sufficed for the exchange flows needed to sustain the deposition of the LE/PLG evaporite cycles. Regarding its potential impacts on terrestrial migrations between Africa and Iberia, however, this small opening would still have presented a sizeable discontinuity of the order of 50 m deep and several km wide.

Regardless of the depositional environment's strong sensitivity to small sea-level changes, as identified above, other arguments based on the timing of the LE/PLG cycles may exclude sea-level control (Krijgsman et al., 1999, 2001; Hilgen et al., 2007). Based on the replacement of pre-MSC precession-related marl–sapropel alternations by gypsum–sapropel alternations in the LE/PLG sequence, these authors infer that the latter are also related to precession-induced Mediterranean climate cycles. They also state that there is not enough time available within the MSC for the LE/PLG cycles to be related to obliquity, and that a glacio-eustatic origin of the cycles may therefore be excluded. However, this argument hinges on a fundamental assumption that sea-level variability would strictly follow obliquity, and this assumption may be seriously flawed. Detailed sea-level records for the Quaternary have revealed the existence of significant sub-orbital sea-level fluctuations, with high rates of both rise and lowering (up to 1 or 2 m per century) and with magnitudes up to 30 m (e.g., Cutler et al., 2003; Siddall et al., 2003, 2004, 2006, in press; Rohling et al., 2004a, 2008; Thompson and Goldstein, 2005; Arz et al., 2007). In the absence of a full understanding of the nature of this sub-orbital variability, it can be neither confirmed nor excluded that similar variability (albeit possibly of smaller amplitude) may have existed during the Late Miocene. Consequently, it remains entirely possible that the LE/PLG cycles might reflect sea-level fluctuations.

Fig. 3 also allows us to test the feasibility of regional climate control on the LE/PLG cycles. Following the line for a sill depth of 48 m from $f_X = 1.0$ down to the lower limit of gypsum saturation, we observe that this point is crossed for $f_X = 0.8$ below which 'normal' marls would be deposited. Analogues of the LE/PLG cycles between gypsum and sapropelic marls could thus be formed by cyclic drops of little more than 20% in the excess evaporation from the Mediterranean. Fig. 3 shows the previously quantified drops in excess evaporation during precession-induced Quaternary humid periods in the Mediterranean that led to the deposition of Holocene sapropel S1 (Rohling, 1999) and Last Interglacial sapropel S5 (Rohling et al., 2004b). Those reductions exceed the inferred drop in excess evaporation needed to explain the gypsum–marl alternations.

Please cite this article as: Rohling, E.J., et al., Controls on Messinian Lower Evaporite cycles in the Mediterranean, Earth Planet. Sci. Lett. (2008), doi:10.1016/j.epsl.2008.08.022

Hence, we find that precession-induced regional climate fluctuations are indeed a feasible mechanism for the observed cycles within the LE/PLG.

We conclude that the LE/PLG evaporite cycles may have resulted from either small (potentially undetectable) sea-level fluctuations, or changes in the Mediterranean hydrological deficit, or a combination of these mechanisms. Although there is a circumstantial case against sea-level control, this is by no means conclusive. If further studies were to reveal sub-orbital sea-level fluctuations during the Messinian (as during the Quaternary), then the accepted astrochronological dating of the LE/PLG duration, and consequently of the other phases of the Messinian Salinity Crisis, might need to be revisited.

Acknowledgements

MS is supported by a Research Council UK Fellowship, the University of Bristol, and the Lamont Doherty Earth Observatory. We thank Andrew Roberts, Harry Bryden, Mike Rogerson, Peter deMenocal, and an anonymous reviewer for helpful comments and suggestions.

Appendix A. to: "Controls on Messinian Lower Evaporite cycles in the Mediterranean" Rohling, E.J., Schiebel, R., Siddall, M.

This appendix consists of two parts. Part 1 is a table of the key parameters used, and Part 2 is an evaluation of the implications of salt extraction by evaporite precipitation in the Mediterranean for the exchange solutions presented in the main text. All the references used are listed in the main text reference list.

Part 1

Key parameters used, in order of appearance in the main text.

Parameter	Description	Units
Q_a	Inflow of Atlantic water into the Mediterranean	$m^3\ s^{-1}$
Q_m	Outflow of Mediterranean water into the Atlantic	$m^3\ s^{-1}$
X	Excess of evaporation over total freshwater input	$m^3\ s^{-1}$
S_a	Salinity (salt content) of Atlantic inflow into the Mediterranean	$g\ kg^{-1}$ (=~$g\ l^{-1}$ =~$kg\ m^{-3}$)
S_m	Salinity (salt content) of Mediterranean outflow into the Atlantic	$g\ kg^{-1}$ (=~$g\ l^{-1}$ =~$kg\ m^{-3}$)
ΔS	$S_m - S_a$	$g\ kg^{-1}$ (=~$g\ l^{-1}$ =~$kg\ m^{-3}$)
f_X	Ratio of past excess evaporation relative to its present-day value ($X_{(1)}/X_{(0)}$)	
f_{Q_a}	Ratio of past inflow relative to its present-day value ($Q_{a(1)}/Q_{a(0)}$)	
Q_{tot}	$Q_a - Q_m$	$m^3\ s^{-1}$
W	Width of the strait cross section	m
D	Depth of the strait cross section	m
g	Acceleration due to gravity	$m\ s^{-2}$
ρ_a	Density of Atlantic inflow into the Mediterranean (NB, for clarity, we follow as close as possible BK91, who express the various density terms in $g\ cm^{-3}$ rather than $kg\ m^{-3}$)	$g\ cm^{-3}$
ρ_m	Density of Mediterranean outflow into the Atlantic (NB, for clarity, we follow as close as possible BK91, who express the various density terms in $g\ cm^{-3}$ rather than $kg\ m^{-3}$)	$g\ cm^{-3}$
n	Ratio of past over modern W and D, so that $n = W_{(1)}/W_{(0)} = D_{(1)}/D_{(0)}$	
Φ	Rate of salt extraction from Mediterranean waters due to evaporite precipitation	$kg\ s^{-1}$
S_{out}	Outflow salinity after accounting for salt extraction from Mediterranean waters	$g\ kg^{-1}$ (=~$g\ l^{-1}$ =~$kg\ m^{-3}$)

Part 2

Evaluation of the implications of salt extraction by evaporite precipitation in the Mediterranean for the exchange solutions presented in the main text.

When salt precipitation takes place in the Mediterranean at a rate of Φ kg s^{-1}, the salt conservation equation presented in main text Eq. (1) becomes

$$Q_{a(1)}S_{a(1)} + Q_{m(1)}S_{out(1)} + \Phi = 0 \tag{a1}$$

so that

$$Q_{m(1)}S_{out(1)} = -Q_{a(1)}S_{a(1)} - \Phi \quad \text{or} \quad Q_{m(1)}S_{out(1)} = Q_{m(1)}S_{m(1)} - \Phi$$

giving

$$S_{out(1)} = S_{m(1)} - \frac{\Phi}{Q_{m(1)}}. \tag{a2}$$

Since $-Q_{m(1)} = Q_{a(1)} + X_{(1)}$, while $Q_{a(1)} = f_{Q_a} Q_{a(0)}$ and $X_{(1)} = f_X X_{(0)}$ Eq. (a2) becomes

$$S_{out(1)} = S_{m(1)} + \frac{\Phi}{\left(f_{Q_a} Q_{a(0)} + f_X X_{(0)}\right)}. \tag{a3}$$

In all of the equations of the main text, which concern the exchange transports at the strait, $S_{m(1)}$ would now need to be replaced by $S_{out(1)}$. With that in mind, main text Eq. (4) can be substituted into Eq. (a3) to give

$$S_{out(1)} = S_{m(1)} + \frac{\Phi}{f_X Q_{a(0)} \cdot \left(\frac{0.05483}{1 - \frac{36.2}{S_{out(1)}}} + \frac{X_{(0)}}{Q_{a(0)}}\right)}. \tag{s4}$$

From main text Eq. (2), we know $X_{(0)}/Q_{a(0)} = \Delta S_{(0)}/S_{m(0)} = 2.1/38.3 = 0.5483$. This allows Eq. (a4) to be simplified and rearranged into

$$S_{m(1)} = S_{out(1)} - \left(\frac{18.238}{f_X} \cdot \frac{\Phi}{Q_{a(0)}} \cdot \frac{1}{\left(\frac{1}{1 - \frac{36.2}{S_{out(1)}}} + 1\right)} \right). \tag{a5}$$

We now need some numbers on the rate of salt deposition (Φ) in kg s^{-1}. Blanc (2000) estimates that a total quantity of 7.88×10^{18} kg was extracted from the Mediterranean throughout the Messinian Salinity Crisis (i.e., between 5.96 and 5.33 Ma, or within 630 kyr); this amounts to $\Phi \approx -400 \times 10^3$ kg s^{-1}. Blanc (2006) reports a smaller estimate for the total quantity, of 6.44×10^{18} kg, but we continue with the highest estimate to assess the maximum impact. Using $Q_{a(0)} \approx 0.95 \times 10^6\ m^3\ s^{-1}$ (Bryden and Kinder, 1991), Eq. (a5) becomes

$$S_{m(1)} = S_{out(1)} + \left(\frac{18.238}{f_X} \cdot \frac{0.42}{\left(\frac{1}{1 - \frac{36.2}{S_{out(1)}}} + 1\right)} \right). \tag{a6}$$

From this, the difference between $S_{m(1)}$ and $S_{out(1)}$ can be worked out for different values of f_X. We find that for $0.1 \le f_X \le 1.5$, Eq. (a6) dictates that, within the halite saturation 'zone', $37.6 < S_{m(1)} - S_{out(1)} < 2.4$. Note that the maximum $S_{m(1)} - S_{out(1)}$ difference would reduce to 7.5 if a lower bound of 0.5 were used for f_X. Halite saturation implies $S > 350$, so that the difference relative to the solutions plotted in main text Fig. 3 would at most be a 10% reduction in the salinity values. The maximum correction would only be about 2% within the more realistic range of $0.5 \le f_X \le 1.5$.

We conclude that, even in the halite 'zone', main text Fig. 3 shows by close approximation the correct solutions despite ignoring salt extraction from the Mediterranean water. Quite simply, salt extraction is not a fast enough process to significantly affect the solutions. This conclusion stands even if we allow a theoretical doubling of the rate of salt precipitation (Φ) through the Messinian Salinity Crisis.

Please cite this article as: Rohling, E.J., et al., Controls on Messinian Lower Evaporite cycles in the Mediterranean, Earth Planet. Sci. Lett. (2008), doi:10.1016/j.epsl.2008.08.022

ARTICLE IN PRESS

References

Arz, H.W., Lamy, F., Ganopolski, A., Nowaczyk, N., Pätzold, J., 2007. Dominant Northern Hemisphere climate control over millennial-scale glacial sea-level variability. Quat. Sci. Rev. 26, 312–321.

Biton, E., Gildor, H., Peltier, W.R., 2008. Red Sea during the Last Glacial Maximum: implications for sea level reconstruction. Paleoceanography 23, PA1214. doi:10.1029/2007PA001431.

Bitzer, K., 2004. Estimating paleogeographic, hydrological and climatic conditions in the upper Burdigalian Vallès-Penedès basin (Catalunya, Spain). Geol. Acta 2, 321–331.

Blanc, P.-L., 2000. Of sills and straits: a quantitative assessment of the Messinian Salinity Crisis. Deep-Sea Res. I 47, 1429–1460.

Blanc, P.-L., 2006. Improved modelling of the Messinian Salinity Crisis and conceptual implications. Palaeogeogr., Palaeoclimatol., Palaeoecol. 238, 349–372. doi:10.1016/j.palaeo.2006.03.033.

Bormans, M., Garrett, C., 1989a. The effects of non-rectangular cross section, friction and barotropic fluctuations on the exchange through the Strait of Gibraltar. J. Phys. Oceanogr. 19, 1543–1557.

Bormans, M., Garrett, C., 1989b. The effect of rotation on the surface inflow through the Strait of Gibraltar. J. Phys. Oceanogr. 19, 1535–1542.

Bryden, H.L., Kinder, T.H., 1991. Steady two-layer exchange through the Strait of Gibraltar. Deep-Sea Res. 38 (suppl. 1), S445–S463.

Bryden, H.L., Stommel, H.M., 1984. Limiting processes that determine basic features of the circulation of the Mediterranean Sea. Oceanol. Acta 7, 289–296.

CIESM, 2008. In: Briand, F. (Ed.), The Messinian Salinity Crisis from Mega-deposits to Microbiology — A Consensus Report. . CIESM Workshop Monographs, vol. 33. Monaco. 168 pp.

Cutler, K.B., Edwards, R.L., Taylor, F.W., Cheng, H., Adkins, J., Gallup, C.D., Cutler, P.M., Burr, G.S., Bloom, A.L., 2003. Rapid sea-level fall and deep-ocean temperature change since the last interglacial period. Earth Planet. Sci. Lett. 206, 253–271. doi:10.1016/S0012-821X(02) 01107-X.

Fairbanks, R.G., 1989. A 17,000-year glacio-eustatic sea level record: influence of glacial melting rates on the Younger Dryas event and deep-ocean circulation. Nature 339, 532–534.

Fairbanks, R.G., 1990. The age and origin of the "Younger Dryas climate event" in Greenland ice cores. Paleoceanography 5, 937–948.

Flecker, R., de Villiers, S., Ellam, R.M., 2002. Modelling the effect of evaporation on the salinity–$^{87}Sr/^{86}Sr$ relationship in modern and ancient marginal-marine systems: the Mediterranean Messinian Salinity Crisis. Earth Planet. Sci. Lett. 203, 221–233.

Garrett, C., Thompson, K., Blanchard, W., 1990. Sea-level flips. Nature 348, 292. doi:10.1038/348292a0.

Hilgen, F., Kuiper, K., Krijgsman, W., Snel, E., van der Laan, E., 2007. Astronomical tuning as the basis for high resolution chronostratigraphy: the intricate history of the Messinian Salinity Crisis. Stratigraphy 4, 231–238.

Hsü, K.J., Ryan, W.B.F., Cita, M.B., 1973. Late Miocene dessication of the Mediterranean. Nature 242, 240–244.

Hsü, K.J., Montadert, L., Bernoulli, D., Cita, M.B., Erickson, A., Garrison, R.E., Kidd, R.B., Mèlieres, F., Müller, C., Wright, R., 1977. History of the Mediterranean salinity crisis. Nature 267, 399–403.

Krijgsman, W., Hilgen, F.J., Raffi, I., Sierro, F.J., Wilson, D.S., 1999. Chronology and progression of the Messinian salinity crisis. Nature 400, 652–655.

Krijgsman, W., Fortuin, A.R., Hilgen, F.J., Sierro, F.J., 2001. Astrochronology for the Messinian Sorbas basin (SE Spain) and orbital (precessional) forcing for evaporite cyclicity. Sediment. Geol. 140, 43–60.

Matthiesen, S., Haines, K., 2003. A hydraulic box model study of the Mediterranean response to postglacial sea-level rise. Paleoceanography 18 (4), 1084. doi:10.1029/2003PA000880.

McCulloch, M.T., De Decker, P., 1989. Sr isotope constraints on the Mediterranean environment at the end of the Messinian salinity crisis. Nature 342, 62–65. doi:10.1038/342062a0.

Meijer, P.Th., 2006. A box model of the blocked-outflow scenario for the Messinian Salinity Crisis. Earth Planet. Sci. Lett. 248, 486–494. doi:10.1016/j.epsl.2006.06.013.

Meijer, P.Th., Krijgsman, W., 2005. A quantitative analysis of the dessication and re-filling of the Mediterranean during the Messinian Salinity Crisis. Earth Planet. Sci. Lett. 240, 510–520. doi:10.1016/j.epsl.2005.09.029.

Nielsen, J.N., 1912. Hydrography of the Mediterranean and adjacent waters. Report of the Danish Oceanographical Expeditions 1908–1910, vol. 1, pp. 77–191.

Pratt, L.J., 1986. Hydraulic control of sill flow with bottom friction. J. Phys. Oceanogr. 16, 1970–1980.

Rohling, E.J., 1999. Environmental controls on salinity and δ18O in the Mediterranean. Paleoceanography 14, 706–715.

Rohling, E.J., Marsh, R., Wells, N.C., Siddall, M., Edwards, N., 2004a. Similar melt–water contributions to glacial sea-level variability from Antarctic and northern ice sheets. Nature 430, 1016–1021. doi:10.1038/nature02859.

Rohling, E.J., Sprovieri, M., Cane, T.R., Casford, J.S.L., Cooke, S., Bouloubassi, I., Emeis, K.C., Schiebel, R., Hayes, A., Jorissen, F.J., Kroon, D., 2004b. Reconstructing past planktic foraminiferal habitats using stable isotope data: a case history for Mediterranean sapropel S5. Mar. Micropaleontol. 50, 89–123. doi:10.1016/S0377-8398(03)00068-9.

Rohling, E.J., Grant, K., Hemleben, Ch., Siddall, M., Hoogakker, B.A.A., Bolshaw, M., Kucera, M., 2008. High rates of sea-level rise during the last interglacial period. Nat. Geosci. 1, 38–42. doi:10.1038/ngeo.2007.28.

Ruggieri, G., Sprovieri, R., 1976. Messinian salinity crisis and its palaeogeographical implications. Palaeogeogr., Palaeoclimatol., Palaeoecol. 20, 13–21.

Siddall, M., Smeed, D., Mathiessen, S., Rohling, E.J., 2002. Modelling the seasonal cycle of the exchange flow in Bab-el-Mandab (Red Sea). Deep-Sea Res. I 49, 1551–1569.

Siddall, M., Rohling, E.J., Almogi-Labin, A., Hemleben, Ch., Meischner, D., Schmeltzer, I., Smeed, D.A., 2003. Sea-level fluctuations during the last glacial cycle. Nature 423, 853–858. doi:10.1038/nature01690.

Siddall, M., Smeed, D.A., Hemleben, Ch., Rohling, E.J., Schmeltzer, I., Peltier, W.R., 2004. Understanding the Red Sea response to sea level. Earth Planet. Sci. Lett. 225, 421–434. doi:10.1016/j.epsl.2004.06.008.

Siddall, M., Bard, E., Rohling, E.J., Hemleben, Ch., 2006. Sea-level reversal during Termination II. Geology 34, 817–820. doi:10.1130/G22705.1.

Siddall, M., Rohling, E.J., Thompson, W.G., Waelbroeck, C., in press. MIS 3 sea-level changes: data synthesis and new outlook, Reviews of Geophysics. doi:10.1029/2007RG000226.

Thompson, W.G., Goldstein, S.L., 2005. Open-system coral ages reveal persistent suborbital sea-level cycles. Science 308 (5720), 401–404. doi:10.1126/science.1104035.

Van Assen, E., Kuiper, K.F., Barhoun, N., Krijgsman, W., Sierro, F.J., 2006. Messinian astrochronology of the Melilla Basin: stepwise restriction of the Mediterranean–Atlantic connection through Morocco. Palaeogeogr., Palaeoclimatol., Palaeoecol. 238, 15–31. doi:10.1016/j.palaeo.2006.03.014.

Waelbroeck, C., Labeyrie, L., Michel, E., Duplessy, J.C., McManus, J.F., Lambeck, K., Balbon, E., Labracherie, M., 2002. Sea-level and deep water temperature changes derived from benthic foraminifera isotopic records. Quat. Sci. Rev. 21, 295–305.

Please cite this article as: Rohling, E.J., et al., Controls on Messinian Lower Evaporite cycles in the Mediterranean, Earth Planet. Sci. Lett. (2008), doi:10.1016/j.epsl.2008.08.022